Dextran-Based Self-Healing Hydrogels Formed by Reversible Diels–Alder Reaction under Physiological Conditions

Zhao Wei, Jian Hai Yang, Xiao Jing Du, Feng Xu, Miklos Zrinyi, Yoshihito Osada, Fei Li,* Yong Mei Chen*

A dextran-based self-healing hydrogel is prepared by reversible Diels–Alder reaction under physiological conditions. Cytocompatible fulvene-modified dextran as main polymer chains and dichloromaleic-acid-modified poly(ethylene glycol) as cross-linkers are used. Both macro- and microscopic observation as well as the rheological recovery test confirm the self-healing property of the dextran-l-poly(ethylene glycol) hydrogels ("l" means "linked-by"). In addition, scanning electrochemical microscopy is used to qualitatively and quantitatively in situ track the self-healing process of the hydrogel for the first time. It is found that the longitudinal depth of scratch on hydrogel surface almost completely healed at 37 °C after 7 h. This work represents a facile approach for fabrication of polysaccharide self-healing hydrogel, which can be potentially used in several biomedical fields.

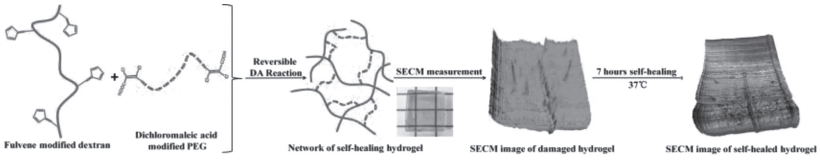

1. Introduction

Hydrogels have been extensively explored as biomaterials recently.[1–3] However, the non-self-healing performance of traditional hydrogels (i.e., the absence of the abilities to automatically repair cracks and regenerate functions) has limited their widespread applications.[4,5] An ideal hydrogel for biomedical applications should have good biocompatibility and nature tissue mimicking feature such as self-healing capability, which is elusive due to the high water content and irreversible chemical cross-links inherent to hydrogels. By endowing hydrogels with self-healing property, they will offer applications in much wider areas, especially in biomedical fields. For instance, self-repairing microcracks inside implanted scaffolds and improved efficiency of drug/cell delivery systems would be promising novel functions.[6,7]

Intense efforts have been devoted to the synthesis of hydrogels with self-healing performance in which two major strategies have been proposed.[8–10] One is based on the usage of noncovalent cross-links like physical interactions including hydrophobic interactions,[11,12] host–guest recognition,[13,14] hydrogen bonds,[15,16] electrostatic interactions,[17,18] or crystallizations.[19] The other approach utilizes dynamic covalent chemistry (DCC) where intrinsic dynamic equilibrium of bond breaking and reformation is responsible for self-healing behavior.[20] Examples

Z. Wei, Dr. J. H. Yang, X. J. Du, Dr. F. Li. Prof. Y. M. Chen
Department of Chemistry, School of Science, MOE Key Laboratory for Non-Equilibrium Synthesis and Modulation of Condensed Matter, Xi'an Jiaotong University, Xi'an 710049, P.R. China
E-mail: feili@mail.xjtu.edu.cn; chenym@mail.xjtu.edu.cn
Z. Wei, Dr. J. H. Yang, X. J. Du, Prof. F. Xu,
Dr. F. Li, Prof. Y. M. Chen
Bioinspired Engineering and Biomechanics Center, Xi'an Jiaotong University, Xi'an 710049, P.R. China
Prof. F. Xu
The Key Laboratory of Biomedical Information Engineering of Ministry of Education, School of Life Science and Technology, Xi'an Jiaotong University, Xi'an 710049, P.R. China
Prof. M. Zrinyi
Laboratory of Nanochemistry, Department of Biophysics and Radiation Biology, Semmelweis University, H-1084, Budapest, Nagyvárad tér 4, Hungary
Prof. Y. Osada
RIKEN 2–1, Hirosawa, Wako, Saitama 351-0198, Japan

DOI: 10.1002/marc.201300494

include phenylboronate ester bonds,[21,22] imine bonds,[6,7] and acylhydrazone bonds etc.[23,24] Although a number of novel self-healing hydrogels have been developed recently, self-healing hydrogels with promising biocompatibility under physiological conditions are still less investigated.

Reversible Diels–Alder (DA) reaction may provide an opportunity for accomplishing this challenge, since the DA reaction has dynamic nature and also belongs to the family of "click" reactions characterized by high yield, high selectivity, and no side reactions.[25–27] It has been used to prepare "click" hydrogels with furan as diene, which have been widely applied as favorable biocompatible materials. Therefore, the hydrogels cross-linked by DA reaction hold the potential to offer both self-healing and biocompatible properties in a single system by combining the advantages of DCC and "click" chemistry. However, there are several challenges associated with the existing self-healing materials based on DA reaction, such as the need of high temperatures (>100 °C) to trigger the reversible DA reaction and poor solubility of functional groups like fulvenes in aqueous solution.[26,28] The ability to self-heal under physiological conditions has not been demonstrated in hydrogels based on DA reactions so far.

To address these challenges, we have developed a facile method to prepare a self-healing hydrogel via reversible DA reaction for the first time. Fulvene-modified hydrophilic dextran (Dex-FE) as dienes and dichloromaleic-acid-modified poly(ethylene glycol) (PEG–DiCMA) as dienophiles are used in preparation. It has been reported that the DA reaction between fulvene and dicyanofumarate units is reversible, which has been used for preparing self-healing organic polymer film, displaying dynamic exchange and self-healing phenomenon at room temperature without external stimuli.[26] Thus, we used dichloromaleic acid that has similar chemical structure as dicyanofumarate to react with fulvene for forming self-healing hydrogels. Dextran is chosen as the main "backbone" of the hydrogel network due to its biocompatible polysaccharide nature and water solubility.[29] PEG is selected as the main chain of cross-linker due to its nontoxicity, excellent water solubility, and easy modification of its hydroxyl terminal groups.[30,31] Such network composed of two different polymer chains connected by chemical bonds is called polymer conetwork.[32,33]

The healing kinetics of the hydrogel was monitored by scanning electrochemical microscopy (SECM) for the first time. By this method, the spatially resolved electrochemical signal allows imaging surface topography. And this in situ observation of the self-healing process has made us possible to determine the healing ratio through the current variation in time and position.

2. Experimental Section

Materials, methods, analysis, and additional experimental data are supplied in the Supporting Information.

3. Results and Discussion

The modified polysaccharide, Dex-FE, was first synthesized by esterification of dextran ($\overline{M}_w$ = 40 000) and 4-(cyclopenta-2,4-dien-1-ylidene) pentanoic acid in the presence of *N,N'*-carbonyldiimidazole (CDI) as activator in DMSO (Scheme S1, Supporting Information). The cross-linker PEG–DiCMA was synthesized from esterification of dichloromaleic anhydride and PEG ($\overline{M}_w$ = 2000) according to the procedures in the literature.[34] The dextran-l-poly(ethylene glycol) (Dex-l-PEG) hydrogel ("l" means "linked-by")[32,33] (with a total concentrations of 20 wt%) can be easily prepared by simply mixing Dex-FE and PEG–DiCMA in phosphate buffer saline (PBS) via DA reaction between fulvene and dichloromaleic acid groups under physiological conditions (pH 7.0, 37 °C). The fluidity of the reaction mixture slowly decreased and brownish yellow color (originates from fulvene of Dex-FE) hydrogels with different molar ratios (R = M_{DiCMA}:M_{FE}) of the functional groups of PEG–DiCMA to Dex-FE were obtained through dynamic covalent DA bonds (Figure 1a,b).

The gelation can be accelerated by increasing the molar ratio of two components in the system. Gelling took 90 min for weakly cross-linked networks when R = 0.5, and gelling time sharply decreased to 15, 10, and 5 min when R was increased to 1, 2, and 3, respectively. However, we observed no hydrogel formation when R < 0.5, which implies there was a lack of necessary cross-links required for attaining the gelation threshold. We also observed that the hydrogels became more opaque with increasing R (Figure 1c–e). To further analyze the transparency difference of the hydrogels, the network structures of freeze-dried hydrogels were investigated by using scanning electron microscopy (SEM). We observed different morphologies and porous structures for hydrogels of different R. Regular micropores were observed in the R = 1 hydrogel (Figure 1c), whereas pore domains became large and nonuniform when R increased to 2 (Figure 1d), and networks became more heterogenous with collapsed micropores when R = 3 (Figure 1e). These structural differences may be attributed to the different gelling times. With increasing R, the gelling time rapidly decreased, resulting in increasingly heterogeneous network structures, which scatter light.[24,35]

The polymer chains in the Dex-l-PEG hydrogel are cross-linked through a reversible DA reaction between Dex-FE and PEG–DiCMA. This cross-linking process exhibits a dynamic equilibrium through ceaselessly uncoupling and

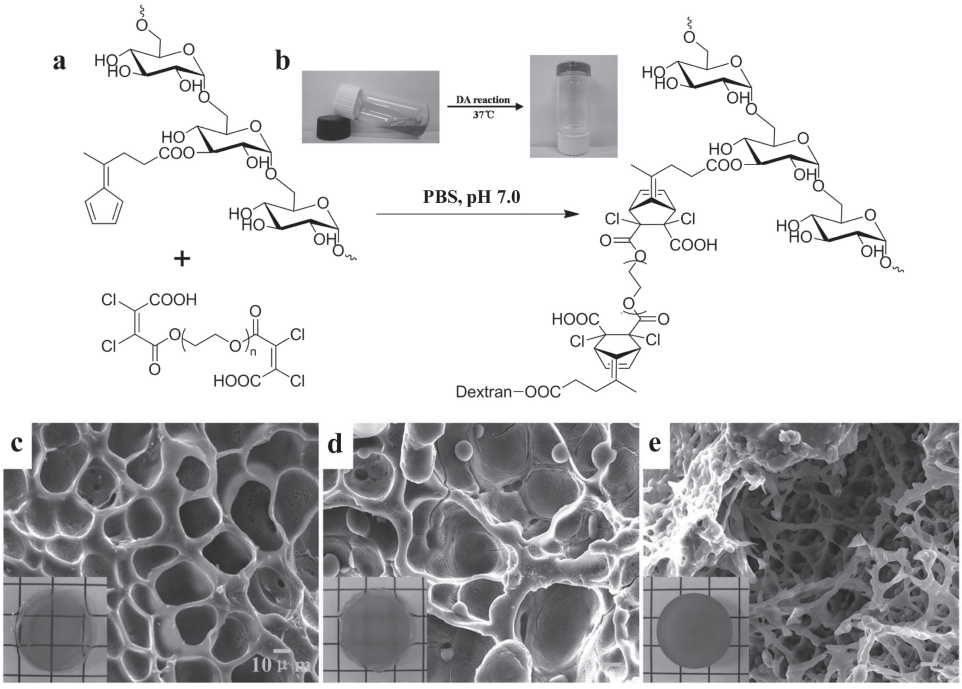

Figure 1. Constructed strategy, SEM images, and photographs of Dex-l-PEG hydrogels. a) Chemical structures of the dextran-based hydrogel cross-linked by reversible Diels–Alder reaction through the fulvene groups of Dex-FE polymeric chains and the two dichloromaleic acid groups at the end of PEG–DiCMA chains. b) The photographs of before and after gelation of Dex-l-PEG hydrogel (20 wt%, R = 1) in PBS (pH 7.0) at 37 °C. c) SEM images and photographs of Dex-l-PEG hydrogels when R = 1, d) R = 2, and e) R = 3. A color version is available in the Supporting Information as Figure S4.

recoupling each of the two functional fulvene and dichloromaleic acid groups. This is the main reason to expect the Dex-l-PEG hydrogels to show self-healing performance. In order to check this expectation, we performed rheological recovery measurements of the hydrogel (Figure 2a,b). From analysis of the rheological yield strain through strain amplitude sweeps at 37 °C, we found that G′ of the Dex-l-PEG hydrogel decreased rapidly at γ = 10% and G′ intersected G″ at γ = 30% (Figure 2a). This data indicate that the network structure of hydrogel is complete but more flowable. With further increase of the strain to 1000%, G′ decreased from about 5000 to 30 Pa, resulting in a fluid-like state hydrogel with collapsed networks. Based on the results from the strain amplitude sweep test, we performed continuous step strain measurements (γ = 1.0% and 1000%) at a frequency of 10 rad s^{-1} at 37 °C to examine the rheology recovery behavior (Figure 2b). Under a 1.0% strain, G′ was larger than G″, indicating the formation of solid-like hydrogel. However, the G′ and G″ values were totally inverted under 1000% strain, indicating that the Dex-l-PEG hydrogels were converted into a fluid-like state. Subsequently, after the strain returned to 1.0% again, G′ and G″ recovered rapidly to their original values and the system returned to its initial solid-like state. Every strain was kept for 300 s and the alternate process of varying strains was repeatable. These results suggest that Dex-l-PEG hydrogel is a novel example of shear-flowing and standing-gelling hydrogels,[36,37] which exhibit very quick recovery of internal networks after a large-amplitude oscillatory breakdown.

In addition, the self-healing behavior of Dex-l-PEG hydrogels was studied by direct visual and mechanical investigation. For this, we halved two disc-shaped hydrogels (one with the original brownish yellow color and the other stained with rhodamine B) using a razor blade to expose fresh surfaces (Figure 2c,d). The two semicircles with fresh surfaces and different colors were placed adjacently along the cut line (Figure 2e). After incubating at 37 °C for 12 h without any external intervention, the boundary of two semicircles blurred and the two pieces merged together into a complete, single hydrogel (Figure 2f). The polymer chains on interfaces of two semicircles have mobility and the reversible DA linkages would recross-link. As a result, the two pieces of hydrogels self-healed at molecular level, which leads to the movement of dye molecules across the interface of the self-healed hydrogel.[6] After healing, we performed a simple mechanical test to check whether adhesion between the surfaces or fusion of cross-links was responsible for the merging of two semicircles into one circular hydrogel disk: the self-healed hydrogel disk was lifted up and deformed under its own weight (Figure 2f). No splitting was observed, demonstrating that the interphase layer was strong enough to sustain its own weight.

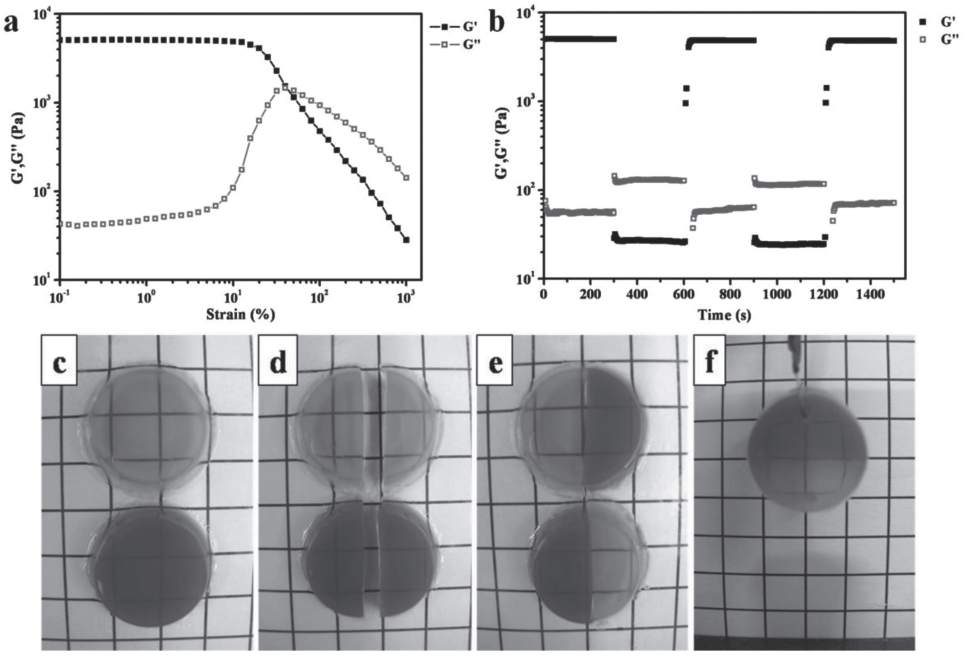

Figure 2. The rheological recovery test and photographs of self-healing process of the Dex-l-PEG hydrogels (20 wt%, R = 1). a) The storage moduli (G') and loss moduli (G'') of the Dex-l-PEG hydrogels from strain amplitude sweep (γ = 1.0%–1000%) at a fixed angular frequency (10 rad s^{-1}) at 37 °C. b) The G' and G'' of the Dex-l-PEG hydrogels from alternate step strain sweep with small strain (γ = 1.0%) for 300 s and following large strain (γ = 1000%) for 300 s at a fixed angular frequency (10 rad s^{-1}) at 37 °C. c) Two Dex-l-PEG hydrogel discs (the red one is colored by rhodamine B). d) The two hydrogel discs were cut into two semicircles. e) The two different colored semicircles were put together for 12 h in a sealed box without any external intervention at 37 °C. f) Merged hydrogel with blur boundary lifted by a tweezers. A color version is available in the Supporting Information as Figure S5.

To further obtain the details of self-healing process, we monitored the self-healing process of hydrogel by using SECM (Figure 3). SECM provides imaging topography data by detecting spatially and temporally resolved electrochemical signals, achieving in situ observation of the detailed self-healing process (e.g., the healing ratio). In this system, SECM image measurements were based on the oxygen reduction reaction ($O_2 + 2\ H_2O + 4e^- = 4OH^-$). The hydrogel acted as an "insulating substrate" to block oxygen diffusion from the bulk aqueous solution to the tip. The smaller the distance from the tip to the hydrogel surface, the lower the oxygen reduction current was as it corresponded to the lower oxygen concentration. On the basis of this principle, the scratched and non-scratched areas of the Dex-l-PEG hydrogel surface have different distances from the Pt microelectrode (i.e. SECM tip) during SECM scanning, which lead to the different oxygen reduction currents. Therefore, the hydrogel morphology in the process of self-healing can be obtained through recording the tip current changes.

To strengthen our SECM results, an optical microscope was used to record the same area scanned by SECM (Figure 3a–c). A sequence of SECM images of the same scratched hydrogel before and after self-healing is shown in Figure 3 (2D images (d–f), 3D images (g–i)). At an initial time (0 h), the scratch on the hydrogel surface was clearly observed in SECM images (Figure 3d,g), which is in accordance with the microscope observation in Figure 3a. The currents corresponding to the scratched line are higher than those to the non-scratched area of the hydrogel, which is because the deep scratch is farther from the tip compared with the non-scratched area of the hydrogel. Then, the currents corresponding to the scratch line at 2 h were lower than those at 0 h (Figure 3e,h). After 7 h, the scratch was finally hardly to observe (Figure 3f,i), which is also consistent with the optical microscope images in Figure 3b,c. This data prove that the longitudinal depth of the scratch effectively healed and almost disappeared without any external stimuli at 37 °C after 7 h. To better express the depth changes of the scratch at different times (0, 2, 7 h), the currents were first averaged from y-axis (0–800 μm) of SECM images, and the resultant average currents were unified by the initial current of 0 h (–0.7375 nA) at the 500th μm of x-axis (Figure 3j). The result shows that the depth extent of scratch, which is expressed by unified current, nearly disappeared after 7 h. The healing ratio of the hydrogel is determined by comparing the scratch depth at different healing times ($(Depth_{0h}–Depth_{healed})/Depth_{0h}$),

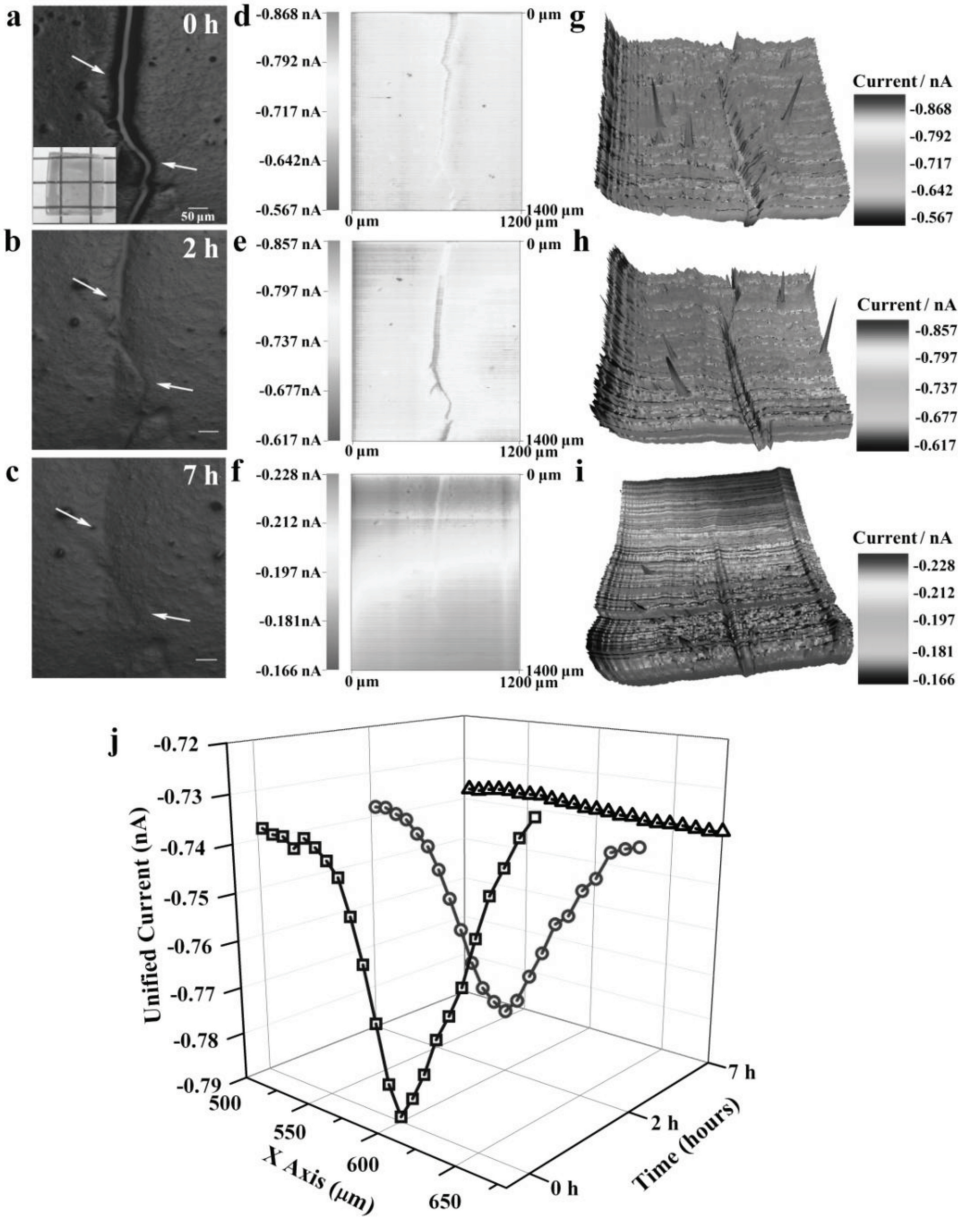

Figure 3. Optical microscope images and corresponding SECM images of the self-healing process of a piece of Dex-l-PEG hydrogel (20 wt%, $R = 1$) with a scratch on its surface for different times. The optical microscope images of the hydrogel with a scratch at (a) 0 h and healed at (d) 2 h and (g) 7 h (scale bar: 50 μm). The arrows indicate the scratch on the hydrogel. 2D and 3D SECM images of the hydrogel with a scratch at (b,c) 0 h and healed at (e,f) 2 h and (h,i) 7 h in 0.1 M KCl aqueous solution. Tip potential: −0.75 V (vs Ag/AgCl RE), tip-hydrogel distances: 10 μm, scan rates: 400 μm s^{-1}. (j) 3D plot of unified currents performed by SECM at different self-healing times of oth, 2nd, and 7th h. A color version is available in the Supporting Information as Figure S6.

which reaches 24.6% at 2 h and ultimately achieves 98.7% after 7 h's healing.

It is worth noting that the shear modulus of Dex-l-PEG hydrogels (ca. 120–5000 Pa) can be attuned to the moduli of naturally soft biological tissues (100–1000 Pa), such as nerve and brain tissues,[38] by adjusting the parameters of R. This indicates that the hydrogels could be modified for various applications within neural tissue engineering and other biomedical fields. Therefore, the cellular compatibility of these novel, self-healing Dex-l-PEG hydrogels was further investigated. For this, we incubated NIH 3T3 fibroblasts with varying concentrations (0–2.0 mg mL^{-1}) of soluble Dex-FE or PEG–DiCMA for 24 h. We did not observe any obvious deleterious effects on cell viability (Figure S3, Supporting Information). Such results demonstrate that compared with the blank control and

dextran or PEG, the Dex-FE and PEG–DiCMA do not show significant cytotoxicity. Our study indicates that both components of self-healing Dex-l-PEG hydrogels are biocompatible, which encourages potential applications in biomedical fields. The 2D culture, 3D encapsulation of 3T3 cells in our novel self-healing hydrogel as well as its in vivo application will be carried out in our follow-up researches.

4. Conclusion

In summary, we report a new straightforward approach for preparing novel dextran-based self-healing hydrogels formed by reversible DA reaction of biocompatible Dex-FE and PEG–DiCMA. Excitingly, the reversible linkages based on DA bonds allow the hydrogels to restructure dynamically and self-heal after mechanical disruption, a phenomenon confirmed by macro/microscopic self-healing performance and rheology recovery measurements. Moreover, SECM was applied for the first time to track in situ and quantitatively characterize the self-healing behavior of hydrogels. In addition, the cellular compatibility test of the components of dextran-based hydrogels indicated that the self-healing hydrogels can be potentially applied in several biomedical fields.

Supporting Information

Supporting Information is available from the Wiley Online Library or from the author.

Acknowledgements: This research was supported by the National Natural Science Foundation of China (Grant 51073127, 51173144, 21105079), the Research Fund for the Doctoral Program of Higher Education of China (Grant 2010–0201110040), the Scientific Research Foundation for the Returned Overseas Chinese Scholars, State Education Ministry, the Fundamental Research Funds for the Central Universities (2009–0109–08140018, 2011-0109-08143038), the International Science & Technology Cooperation Program supported by Ministry of Science and Technology of China and Shaanxi Province, and New Research Support Project of Xi'an Jiaotong University, P. R. China. F.X. was also partially supported by the Major International Joint Research Program of China (11120101002), the National 111 Project of China (B06024), and International Science & Technology Cooperation Program of China (2013DFG02930).

Received: 28 June, 2013; Revised: 17 July, 2013; Published online: August 9, 2013; DOI: 10.1002/marc.201300494

Keywords: dextran; hydrogels; self-healing

[1] E. S. Place, J. H. George, G. K. Williams, *Chem. Soc. Rev.* **2009**, *38*, 1139.
[2] Y. Shigekura, Y. M. Chen, H. Furukawa, T. Kaneko, D. Kaneko, Y. Osada, J. P. Gong, *Adv. Mater.* **2005**, *17*, 2699.
[3] Y. M. Chen, R. Ogawa, A. Kakugo, Y. Osada, J. P. Gong, *Soft Matter* **2009**, *5*, 1084.
[4] K. Dong, Z. Wei, Z. M. Yang, Y. M. Chen, *Sci. China: Chem.* **2012**, *42*, 741.
[5] A. B. W. Brochu, S. L. Craig, W. M. Reichert, *J. Biomed. Mater. Res. A* **2011**, *96*, 492.
[6] Y. L. Zhang, L. Tao, S. X. Li, W. Wei, *Biomacromolecules* **2011**, *12*, 2894.
[7] B. Yang, Y. L. Zhang, X. Y. Zhang, L. Tao, S. X. Li, W. Wei, *Polym. Chem.* **2012**, *3*, 3235.
[8] Y. Amamoto, H. Otsuka, A. Takahara, K. Matyjaszewski, *Adv. Mater.* **2013**, *24*, 3975.
[9] M. W. Urban, *Nat. Chem.* **2012**, *4*, 80.
[10] F. Herbst, D. Dohler, P. Michael, W. H. Binder, *Macromol. Rapid Commun.* **2013**, *34*, 203.
[11] D. C. Tuncaboylu, M. Sahin, A. Argun, W. Oppermann, O. Okay, *Macromolecules* **2012**, *45*, 1991.
[12] G. Akay, A. Hassan-Raeisi, D. C. Tuncaboylu, N. Orakdogen, S. Abdurrahmanoglu, W. Oppermann, O. Okay, *Soft Matter* **2013**, *9*, 2254.
[13] M. Nakahata, Y. Takashima, H. Yamaguchi, A. Harada, *Nat. Commun.* **2011**, *2*, 511.
[14] T. Kakuta, Y. Takashima, M. Nakahata, M. Otsubo, H. Yamaguchi, A. Harada, *Adv. Mater.* **2013**, *25*, 2849.
[15] A. Phadke, C. Zhang, B. Arman, C.-C. Hsu, R. A. Mashelkar, A. K. Lele, M. J. Tauber, G. Arya, S. Varghese, *Proc. Natl. Acad. Sci. USA* **2012**, *109*, 4383.
[16] A. Campo, J. Cui, *Chem. Commun.* **2012**, *48*, 9302.
[17] Q. Wang, J. L. Mynar, M. Yoshida, E. Lee, M. Lee, K. Okuro, K. Kinbara, T. Aida, *Nature* **2010**, *463*, 339.
[18] K. Haraguchi, K. Uyama, H. Tanimoto, *Macromol. Rapid Commun.* **2011**, *32*, 1253.
[19] A. P. Nowak, V. Breedveld, L. Pakstis, B. Ozbas, D. J. Pine, D. Pochan, T. J. Deming, *Nature* **2002**, *417*, 424.
[20] S. J. Rowan, S. J. Cantrill, G. R. L. Cousins, J. K. M. Sanders, J. F. Stoddart, *Angew. Chem Int. Ed.* **2002**, *41*, 898.
[21] M. C. Roberts, M. C. Hanson, A. P. Massey, E. A. Karren, P. F. Kiser, *Adv. Mater.* **2007**, *19*, 2503.
[22] L. He, D. E. Fullenkamp, J. G. Rivera, P. B. Messersmith, *Chem. Commun.* **2011**, *47*, 7497.
[23] G. H. Deng, C. M. Tang, F. Y. Li, H. F. Jiang, Y. M. Chen, *Macromolecules* **2010**, *43*, 1191.
[24] G. H. Deng, F. Y. Li, H. X. Yu, F. Y. Liu, C. Y. Liu, W. X. Sun, H. F. Jiang, Y. M. Chen, *ACS Macro Lett.* **2012**, *1*, 275.
[25] X. X. Chen, M. A. Dam, K. Ono, A. Mal, H. B. Shen, S. R. Nutt, K. Sheran, F. Wudl, *Science* **2002**, *295*, 1698.
[26] P. Reutenauer, E. Buhler, P. J. Boul, S. J. Candau, J.-M. Lehn, *Chem. Eur. J.* **2009**, *15*, 1893.
[27] C. M. Nimmo, S. C. Owen, M. S. Shoichet, *Biomacromolecules* **2011**, *12*, 824.
[28] B. J. Adzima, C. J. Kloxin, C. N. Bowman, *Adv. Mater.* **2010**, *22*, 2784.
[29] G. M. Sun, X. J. Zhang, Y.-I. Shen, R. Sebastian, L. E. Dickinson, K. F. Talbot, M. Reinblatt, C. Steenbergen, J. W. Harmon, S. Gerech, *Proc. Natl. Acad. Sci. USA* **2011**, *108*, 20976.
[30] B. Ozcelik, K. D. Brown, A. Blencowe, M. Daniell, G. W. Stevens, G. G. Qiao, *Acta Biomaterialia* **2013**, *9*, 6594.
[31] N. T. Huynh, Y. S. Jeon, D. Kim, J. H. Kim, *Polymer* **2013**, *54*, 1341.

[32] Cs. Fodor, G. Kali, B. Iván, *Macromolecules* **2011**, *44*, 4496.
[33] Cs. Fodor, A. Domján, B. Iván, *Polym. Chem.* **2013**, *4*, 3714.
[34] M. Bonini, S. Lenz, R. Giorgi, P. Baglioni, *Langmuir* **2007**, *23*, 8681.
[35] H. Takeshita, T. Kanaya, K. Nishida, K. Kaji, *Phys. B: Condens. Matter* **2002**, *311*, 78.
[36] X. Y. Hou, D. Gao, J. L. Yan, Y. Ma, K. Q. Liu, Y. Fang, *Langmuir* **2011**, *27*, 12156.
[37] K.-I. Sano, R. Kawamura, T. Tominaga, N. Oda, K. Ijiro, Y. Osada, *Biomacromolecules* **2011**, *12*, 4173.
[38] J. L. Vanderhooft, B. K. Mann, G. D. Prestwich, *Biomacromolecules* **2007**, *8*, 2883.